Research Article

The temperature distribution of the wet cylinder liner of v-12 engine according to calculation and experiment

Kien Nguyen TRUNG[1,2,*]

[1]Faculty of Vehicle and Energy Engineering, PHENIKAA University, Hanoi 12116, Vietnam
[2]PHENIKAA Research and Technology Institute (PRATI), A&A Green Phoenix Group JSC, No.167 Hoang Ngan, Trung Hoa, Cau Giay, Hanoi 11313, Vietnam

ABSTRACT

In order to serve the design, improvement, and manufacture of engine cylinder liners, it is necessary to accurately determine its temperature distribution. This paper presents the calculation of the cylinder liner temperature distribution in a V-12 engine by the finite element method (FEM) written in ANSYS Parametric Design Language (APDL) and verified with experimental results. In this model, the process of heat transfer from the ring group and area of the piston skirt to the cylinder liner wall is considered by using the thermal circuit method. In the study, at engine speeds of 2000 [rev/min] and 1200 [rev/min], the thermal distribution of the cylinder liner is carried out at 50%, 60%, 75%, and 100% of an entire load. The results of the tests show that the theoretical model is highly reliable, with the largest relative error of 5.49%.

Cite this article as: Trung KN. The temperature distribution of the wet cylinder liner of v-12 engine according to calculation and experiment. J Ther Eng 2021:7:Supp 14:1872–1884.

INTRODUCTION

In reciprocating internal combustion engines, the heat transfer from hot gases to coolant exhibits from 25 percent to 30 percent of the total energy released during burning the fuel-air mixture. The total heat dissipation to the cooling fluid depends mainly on the type of engine and the operating conditions. About half of the heat is transferred to the cylinder liner walls, and most of the remaining heat goes to the coolant in the cylinder head, with the highest rates around the exhaust valves. The lubricating oil also indirectly transfers heat from the hot gases to the coolant [1].

In Ref. [2], a number of empirical models for predicting in-cylinder heat transfer in internal combustion engines have been investigated. That investigation has shown that, even after several decades, the main difficulty remains the right selection of the significant parameters, specifically flow velocity, characteristic length, and fluid properties. Because the entire flow and thermal distribution in the cylinder, particularly in the boundary layer, cannot be fully

---

interpreted by analytical methods, the selection of these quantities is still based on empirical approaches.

The significance of heat transfer to the combustion chamber wall of internal combustion engines has been recognized, and the results of various theoretical and experimental research efforts on this issue have been presented in the literature. However, it is acknowledged that the problem is quite difficult, and many of its aspects have not been extensively examined up to this moment [3–5]. In recent years, there has been a surge in interest in heat transfer phenomena in internal combustion engines, owing to their importance in, among other things, successful simulations of thermodynamic cycles and investigations of thermal loading of the components at critical areas [3–5].

Thermal losses are one of three major factors to consider when optimizing the performance of internal combustion engines, accounting for 50 ÷ 60% total losses, according to Richardson [6]. To minimize thermal losses, the cylinder wall temperature should ideally be kept close to the temperature of the combustion gases inside the cylinder. In thermodynamic control-oriented modeling of cycle-to-cycle exhaust gas temperature, the cylinder liner temperature plays a significant role. Dehghani Firoozabadi et al [7] emphasized the significance of defining the cylinder wall temperature in order to improve such models. Besides, in terms of emission levels, Wang and Stone [8] demonstrated that the cylinder wall temperature influences Hydrocarbon (HC) and Nitrogen Oxide (NO_x) emissions from IC engines. It has been demonstrated that higher liner temperatures reduce HC emissions, whereas the opposite is typically true for NO_x emissions. As a result, the optimal temperature of the cylinder liner wall should be sought based on a desired (weighted) trade-off between HC and NO_x emissions. The piston-cylinder system is responsible for the vast majority of all losses and emissions. As a result, an integrated approach, particularly one with predictive capabilities, is required. R. Rahmani [9] et al. demonstrated that cylinder liner temperature is critical in reducing hydrocarbon (HC) and nitrogen oxide (NOx) emissions from the compression ring-cylinder liner conjunction. The findings imply that there is an optimum range for liner working temperature that is independent of engine speed in order to minimize frictional losses. Controlling liner temperature, in conjunction with the study of NOx and HC emissions, can help to mitigate frictional power loss and reduce emissions.

Caglar Dere and Cengiz Deniz [10] showed that keeping the cylinder liner temperature at the maximum continuous rating temperature has respectable efficiency benefits under various operating loads. With the results were shown in the study, a 0.5 percent reduction in fuel consumption could be achieved, resulting in 127.8 tons of fuel and 398 tons of CO_2 reduction in a year. Furthermore, waste heat recovery system calculations were performed, and it was discovered that an additional 48.8 tons of fuel could be saved in the generation of electricity. As a result, controlled cylinder wall temperatures can be regarded as one of the methods for resolving ship efficiency and emission issues in the near future.

P. Gustof, A. Hornik [11] completed the determination of the temperature distribution in the wet cylinder sleeve during the initial phase of the turbo diesel engine. The two-zone combustion model and the finite element method were used to obtain the results. According to the results of the calculations, the maximum temperature of the wet cylinder sleeve in the 40s of engine operation is around 444 [K]. The calculations revealed that the cylinder sleeve heats up the fastest during the first 20 seconds of engine operation (on average about 3 [K] per second), after which the temperature begins to stabilize and changes in a small range in 40 seconds (about 0.7 [K] per second). The numerical simulations demonstrated the feasibility of employing the original two-zone combustion model and finite element method to analyze the temporary temperature distribution on individual cylinder surfaces.

Engine cylinder heat transfer is one of the most important processes in internal combustion engines, but despite decades of research, a satisfactory understanding remains elusive. The engine head and valve seats provide approximately 50% of the heat flow to the engine coolant, the cylinder sleeve or walls provide 30%, and the exhaust port area provides the remaining 20% [12]. A variety of methods can be used to model the heat transfer processes in an internal combustion engine. From simple thermal networks to multidimensional differential equation modeling, these techniques are available. The modeling method chosen must take into account factors such as the computational accuracy required and the data available to model the engine configuration and operation [12].

The V-12 engine is a high-speed diesel engine with cooling water regularly. The engine is made up of 12 cylinders arranged in a V-shape with a 60^0 angle between their axes [13] and is used on Russian and Vietnamese Tanks. These engines have high durability and are not turbocharged, so to improve their power density and efficiency, one of the proposed solutions is to use a supercharging system with exhaust gas energy recovery, known as an exhaust gas turbocharger. When turbocharging, an issue of concern is the mechanical heat stress of the components of the combustion chamber. Besides, in the process of engine operation, the wet cylinder liners are often damaged by the wear and tear of cooling water so they are often repaired by the replacement method. When designing a cylinder liner, it is necessary to determine the thermal load, the mechanical load acting on during the engine operating cycle, including determining the temperature distribution of the cylinder liner. Therefore, accurate cylinder liner temperature distribution is required for cylinder optimum design, fatigue analysis, and studying development. Heat transfer analysis is also important in engine design, accurate prediction of temperature distribution is required for the analysis of

thermal stress limits for cylinder materials. Accurate prediction of heat flux, in particular, is useful for determining the cylinder chamber geometry to minimize emissions [1,9]. When turbocharging, due to changing the amount of fuel injected per cycle so that the amount of heat transferred to the cylinder liner also increases. Therefore, the accurate determination of the temperature distribution of a cylinder liner is an important research content to determine the maximum boost pressure ratio for this engine. The content of the paper includes the calculation results of the temperature distribution of the wet cylinder liner, as well as a comparison with experimental results.

METHODOLOGY

To calculate the amount of heat transferred to the cylinder wall, the temperature and heat transfer coefficient of the in-cylinder gases must be calculated, which necessitates the calculation of the engine operating cycle. The simulation of the working cycle of the V-12 engine is made by GT-Power at 50 percent, 60 percent, 70 percent, and 100 percent load at engine speeds of 1200 [rev/min] and 2000 [rev/min]. Because the engine operates at its maximum rated power and torque at these speeds. The temperature distribution in the components that surround the chamber is affected by engine variables such as engine speed, engine load, overall equivalence ratio, and compression ratio,… etc [1,14,15]. Speed and load have the greatest influence comparison with other variables. Experimentation was used to validate the engine simulation model, as detailed in Ref. [16]. The results of calculating the gas temperature and heat transfer coefficient from engine simulation are

used to determine the III kind boundary conditions of the cylinder liner, and then the temperature distribution of the wet cylinder liner is calculated using the finite element method.

To calculate V-12 engine cylinder temperature field, the author built a calculation program in the form of APDL based on the finite element method written as jobname. txt, then run by ANSYS software [17]. In order to match the evaluation with the experimental results, the heat transfer is assumed to be quasi-steady [1]. To determine the boundary conditions of the heat exchange coefficient and temperature as input parameters when calculating the temperature field by finite element method (FEM) based on ANSYS software the author divides the heat exchanger surfaces of the cylinder liner into the areas shown in Figure 1. These areas are divided based on the calculation of the engine operating cycle, the correlation between the piston surface and cylinder wall when the piston is at the bottom dead center (BDC). In this model, the process of heat transfer (heat conduction) from the ring group and the piston skirt area to the cylinder liner wall is considered by using the thermal circuit method (see Ref. [11,12,16,18,19] for more detail).

The heat exchange process included:

+ The process of heat exchange between the in-cylinder gases and cylinder wall, (α_1, T_1);
+ The cylinder wall surface takes into account the process of heat exchange between the in-cylinder gases and the cylinder wall, conduction from the ring land to the cylinder wall, (α_2, T_2);
+ The cylinder wall surface takes into account the process of heat exchange between the in-cylinder gases and the cylinder wall, conduction from the ring land and the piston skirt region to the cylinder wall, (α_3, T_3);
+ The cylinder wall surface takes into account the process of heat exchange between the in-cylinder gases and the cylinder wall, conduction from the ring land and the skirt region to the cylinder wall, and the heat exchange between the blow-by gas and the cylinder wall $(\alpha_4, T_4, \alpha_5, T_5, \alpha_6, T_6, \alpha_7, T_7)$;
+ The cylinder wall surface takes into account the process of exchanging heat between the skirt region and the cylinder wall, between the blow-by gas with the cylinder wall (α_8, T_8);
+ The cylinder wall refers to the process of the heat exchange between the cylinder sleeve and the blow-by gas, (α_9, T_9);
+ The conduction between the cylinder sleeve and the engine block, (α_{10}, T_{10});
+ The convection between the cylinder sleeve and the cooling water, (α_{11}, T_{11});
+ The conduction between the cylinder sleeve and the engine block, (α_{12}, T_{12}).

Table 1. V-12 diesel engine specifications [13]

| Parameters	Symbol	Value	Unit
Number of cylinders	i	12	-
Engine type	V-12	Diesel, the vee (V) arrangement, the twelve cylinders are arranged in two banks of six, with a 60^0 angle between their axes.	
Firing order		1^L-6^R-5^L-2^R-3^L-4^R-6^L-1^R-2^L-5^R-4^L-3^R	
Compression ratio	ε	15±0.5	
Max. power	$N_{e.max}$	520≈387.4	[HP] [kW]
Engine speed at the max. power	n_N	2000	[rev/min]
Max. torque	$M_{e.max}$	2256.3±10	[N.m]
Engine speed at the max. torque	n_M	1200	[rev/min]
Specific fuel consumption	$G_{e.min}$	265±5	[g/kW.h]
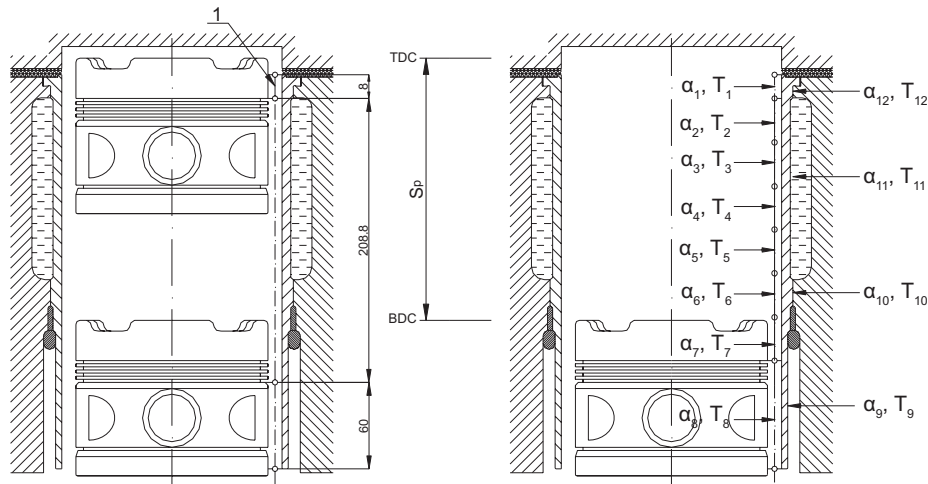
Figure 1. Surfaces of the heat exchange of the wet cylinder liner.

The average heat transfer coefficient and temperature of the in-cylinder gases in the whole cycle are determined as follows:

$$\overline{\alpha_\Sigma} = \frac{1}{720}\int_0^{720} \alpha.d\varphi, \ [\text{W/m}^2.\text{K}] \tag{1}$$

$$\overline{T_\Sigma} = \frac{1}{720.\overline{\alpha_\Sigma}}\int_0^{720} \alpha.T.d\phi, \ [\text{K}] \tag{2}$$

with: j – crank angle, [degrees], α – heat transfer coefficient, [W/m^2.K], T – the temperature of the in-cylinder gases, [K].

The heat transfer coefficient, the temperature, and pres-sure of the in-cylinder gases according to the crank angle are determined when running a simulation model built by GT-Power software. Based on the calculation results and by the method of graph integration, we can determine the values of heat transfer coefficient (α_i – [W/m^2.K]) and the temperature corresponding to each region of the cylinder liner (T_i – [K]) due to exposure to the in-cylinder gases. Furthermore, the heat transfer coefficient and tempera-ture on the cylinder mirror surface as a result of the heat transfer process from the surface side of the piston over top compression ring to the cylinder liner were calculated [11,18]:

$$\alpha_1 = \frac{1}{2}\left[\frac{1}{120}\left(\int_{360}^{390}\alpha d\varphi + \int_{-30}^{0}\alpha d\varphi + \int_{0}^{30}\alpha d\varphi + \int_{330}^{360}\alpha d\varphi\right)\right]$$

$$= \frac{1}{2}\left[\frac{1}{120}\left(\int_{330}^{390}\alpha d\varphi + \int_{-30}^{30}\alpha d\varphi\right)\right][\text{W/m}^2.\text{K}]$$

$$T_1 = 0.8\left[\frac{1}{120.\alpha_1}\left(\int_{330}^{390}\alpha.Td\varphi + \int_{-30}^{30}\alpha.Td\varphi\right)\right] [\text{K}]$$

$$\alpha_2 = \frac{1}{2}\left[\frac{1}{120}\left(\int_{390}^{420}\alpha d\varphi + \int_{-60}^{-30}\alpha d\varphi + \int_{30}^{60}\alpha d\varphi + \int_{300}^{330}\alpha d\varphi\right)\right][\text{W/m}^2.\text{K}]$$

$$T_2 = 0.8\left[\frac{1}{120.\alpha_2}\left(\int_{390}^{420}\alpha.Td\varphi + \int_{-60}^{-30}\alpha.Td\varphi + \int_{30}^{60}\alpha.Td\varphi \right.\right.$$
$$\left.\left. + \int_{300}^{330}\alpha.Td\varphi\right)\right][\text{K}]$$

$$\alpha_3 = \frac{1}{2}\left[\frac{1}{120}\left(\int_{420}^{450}\alpha d\varphi + \int_{-90}^{-60}\alpha d\varphi + \int_{60}^{90}\alpha d\varphi + \int_{270}^{300}\alpha d\varphi\right)\right][\text{W/m}^2.\text{K}]$$

$$T_3 = 0.8\left[\frac{1}{120.\alpha_3}\left(\int_{420}^{450}\alpha.Td\varphi + \int_{-90}^{-60}\alpha.Td\varphi + \int_{60}^{90}\alpha.Td\varphi \right.\right.$$
$$\left.\left. + \int_{270}^{300}\alpha.Td\varphi\right)\right][\text{K}]$$

$$\alpha_4 = \frac{1}{2}\left[\frac{1}{120}\left(\int_{450}^{480}\alpha d\varphi + \int_{-120}^{-90}\alpha d\varphi + \int_{90}^{120}\alpha d\varphi + \int_{240}^{270}\alpha d\varphi\right)\right][\text{W/m}^2.\text{K}]$$

$$T_4 = 0.8\left[\frac{1}{120.\alpha_4}\left(\int_{450}^{480}\alpha.Td\varphi + \int_{-120}^{-90}\alpha.Td\varphi + \int_{90}^{120}\alpha.Td\varphi \right.\right.$$
$$\left.\left. + \int_{240}^{270}\alpha.Td\varphi\right)\right][\text{K}]$$

$$\alpha_5 = \frac{1}{2}\left[\frac{1}{120}\left(\int_{480}^{510}\alpha d\varphi + \int_{-150}^{-120}\alpha d\varphi + \int_{120}^{150}\alpha d\varphi + \int_{210}^{240}\alpha d\varphi\right)\right][\text{W/m}^2.\text{K}]$$

$$T_5 = 0.8\left[\frac{1}{120.\alpha_5}\left(\int\limits_{480}^{510}\alpha.Td\varphi + \int\limits_{-150}^{-120}\alpha.Td\varphi + \int\limits_{120}^{150}\alpha.Td\varphi + \int\limits_{210}^{240}\alpha.Td\varphi\right)\right][K]$$

$$\alpha_6 = \frac{1}{2}\left[\frac{1}{120}\left(\int\limits_{510}^{540}\alpha d\varphi + \int\limits_{-180}^{-150}\alpha d\varphi + \int\limits_{150}^{180}\alpha d\varphi + \int\limits_{180}^{210}\alpha d\varphi\right)\right][W/m^2.K]$$

$$= \frac{1}{2}\left[\frac{1}{120}\left(\int\limits_{510}^{540}\alpha d\varphi + \int\limits_{-180}^{-150}\alpha d\varphi + \int\limits_{150}^{210}\alpha d\varphi\right)\right][W/m^2.K]$$

$$T_6 = 0.8\left[\frac{1}{120.\alpha_6}\left(\int\limits_{510}^{540}\alpha.Td\varphi + \int\limits_{-180}^{-150}\alpha.Td\varphi + \int\limits_{150}^{210}\alpha.Td\varphi\right)\right][K]$$

With the defined boundary conditions, through the program for calculating the temperature distribution of cylinder liner written in APDL format, for more detail, the program can be referenced in appendix and Ref. [16].

EXPERIMENTAL SET-UP

Measuring technique

To determine the temperature distribution of the cylinder liner, we can use direct measurement methods by employing a measurement technique by using thermocouples at a specific location, which was likely to achieve the local temperatures. To facilitate processing and avoid damage to the sensor, the temperature measurement position at 8 characteristic points on the cylinder sleeve is shown in Figure 2 and Figure 3.

Select cylinder temperature measuring device

With the characteristics of the thermocouples and based on the temperature range of the cylinder sleeve to be measured, the specific structure of the cylinder liner and the water jacket on the engine block. The author chooses Omega T-type thermocouples for our experimental research work. Thermocouples include 2 types: TTCP polar (+) and TTCC polar (-) with a diameter of 0.08 mm to form a thermocouple, this type of thermocouple is shown in Figure 3 [16].

The connection diagram and wiring diagram in the temperature measurement system at the feature locations in the engine cylinder liner are shown in Figure 4 and Figure 5.

Facilities for testing

The experiments were carried out in one of the engine test cells of Factory Z153 - the General Department of Techniques, Vietnam Ministry of National Defense. The computer systems were housed in the control room of the test cell. Collect measurement data on the display devices while the engine is in a stable operating mode.
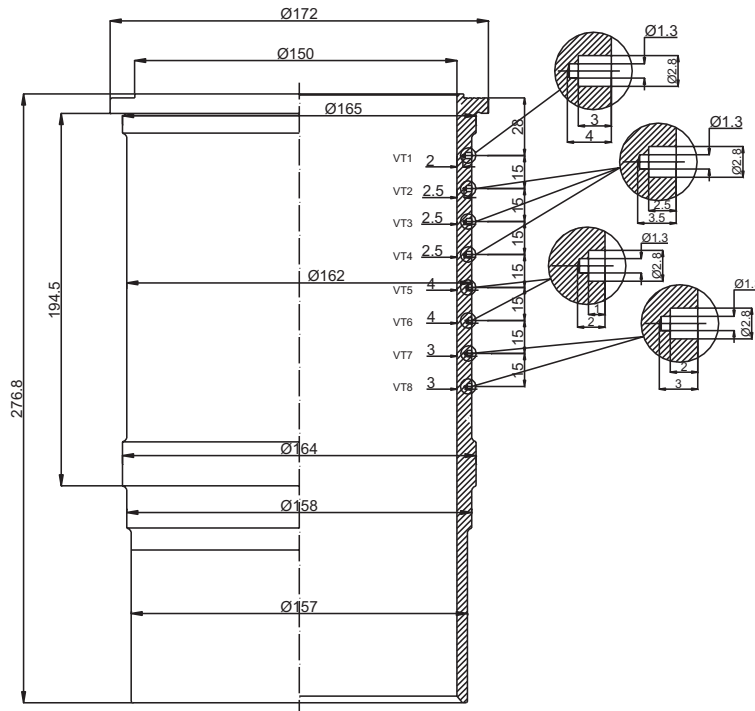

Figure 2. Schematic location of thermocouple sets in the wet cylinder liner.

Figure 3. The location of thermocouple sets in the wet cylinder liner is depicted schematically.

RESULTS AND DISCUSSION

Through running the program written by The ANSYS Parametric Design Language (APDL) in the appendix, we get the results in different speeds and loads as shown in figures from Figure 6 to Figure 13. In this calculation model, twelve characteristics of the heat transfer surfaces were identified in calculating the thermal distribution of the wet cylinder liner (Figure 1), and definite boundary conditions values of type III were assigned to them. Then, the Ansys model will be validated by experiment (Figure 14 and Figure 15).

The calculated results demonstrate how temperature varies along the length of the cylinder liner of a V-12 diesel engine. From these results, the highest temperature area is the top inside edge of the cylinder liner. The temperature distribution decreases gradually from the mirror surface to
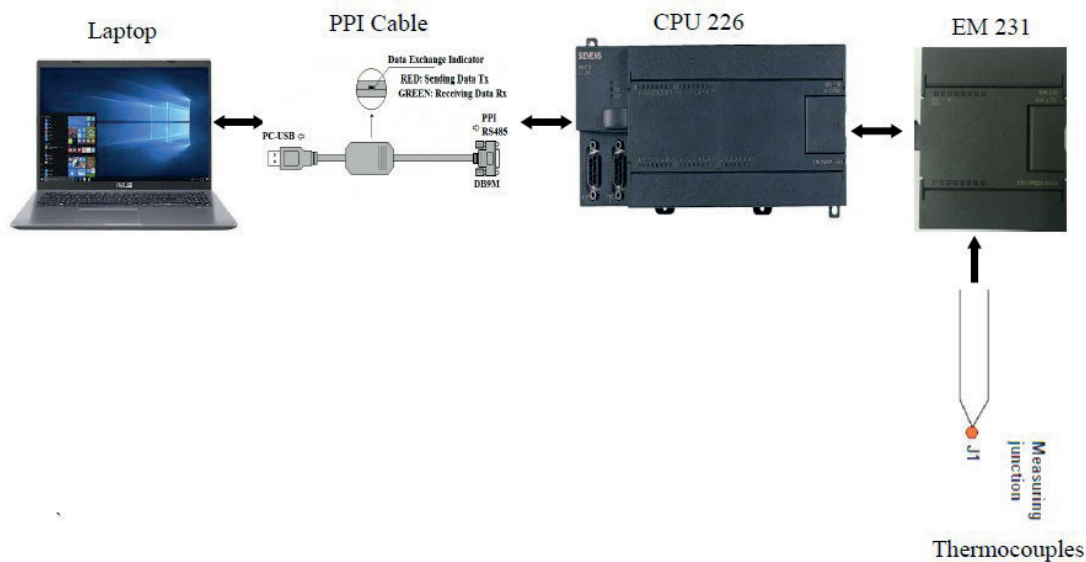

Figure 4. Connection diagram of the temperature measurement system of the feature locations in the engine cylinder liner.
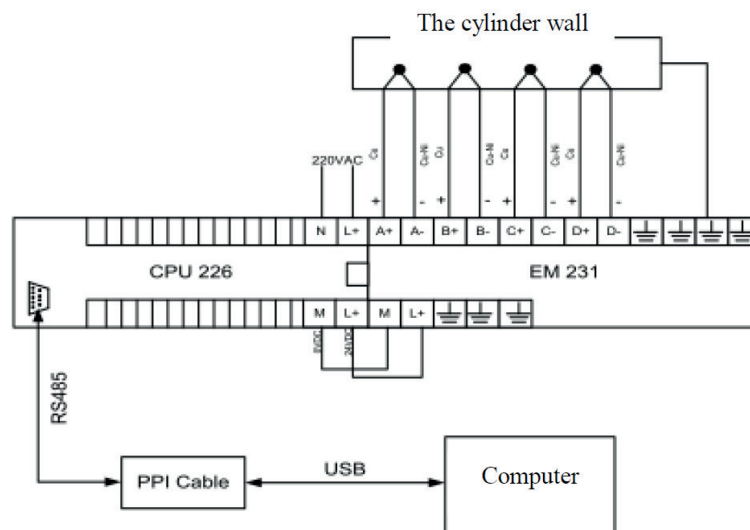

Figure 5. Wiring diagram of the temperature measurement system of feature locations in the engine cylinder liner.
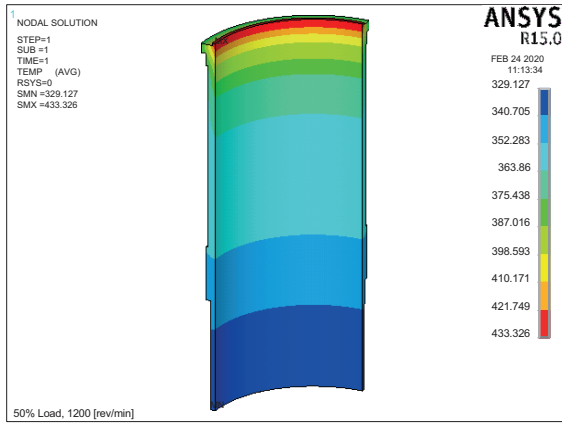
Figure 6. The cylinder liner temperature distribution at 50% load, 1200 rev/min.
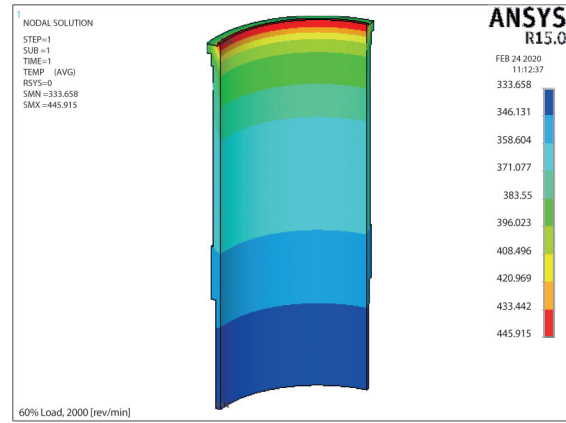

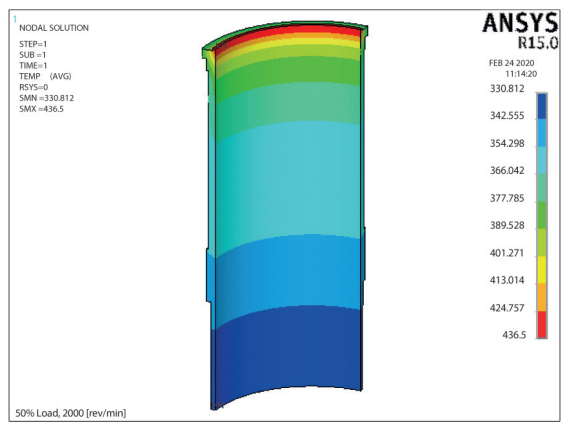**Figure 9.** The cylinder liner temperature distribution at 60% load, 2000 rev/min.

Figure 7. The cylinder liner temperature distribution at 50% load, 2000 rev/min.
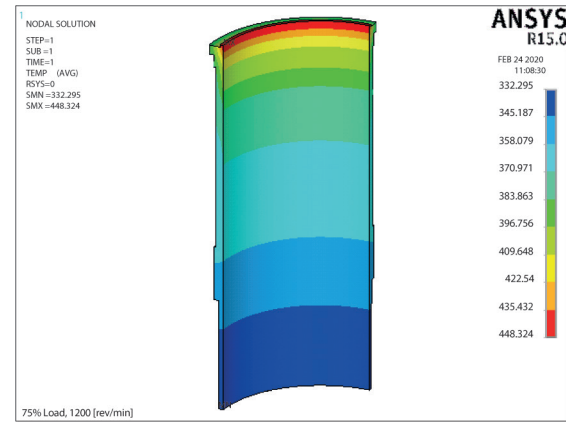

Figure 10. The cylinder liner temperature distribution at 75% load, 1200 rev/min.

Figure 8. The cylinder liner temperature distribution at 60% load, 1200 rev/min.

Figure 11. The cylinder liner temperature distribution at 75% load, 2000 rev/min.
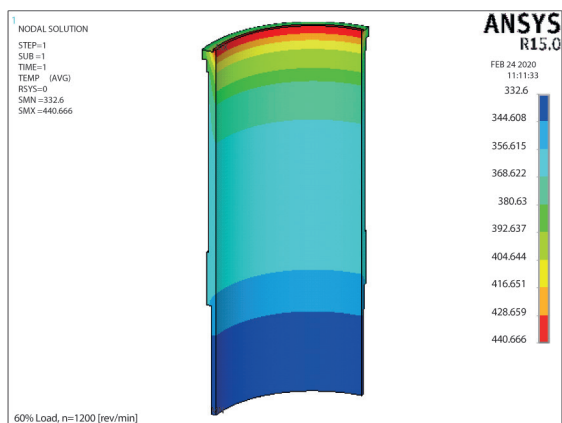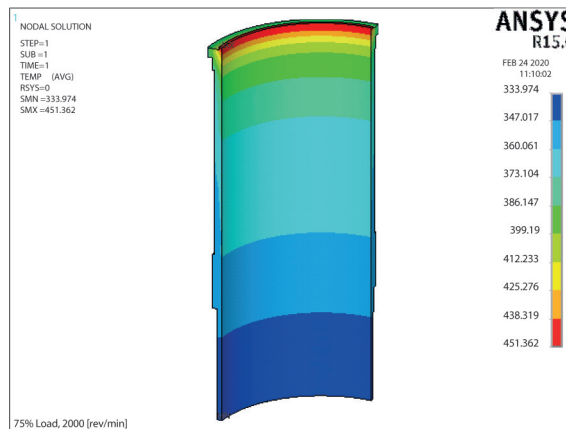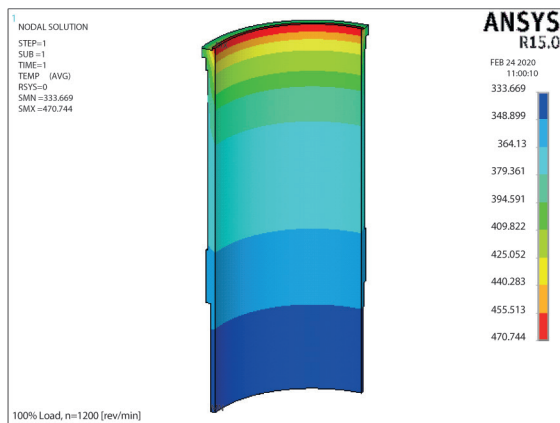
Figure 12. The cylinder liner temperature distribution at 100% load, 1200 rev/min.
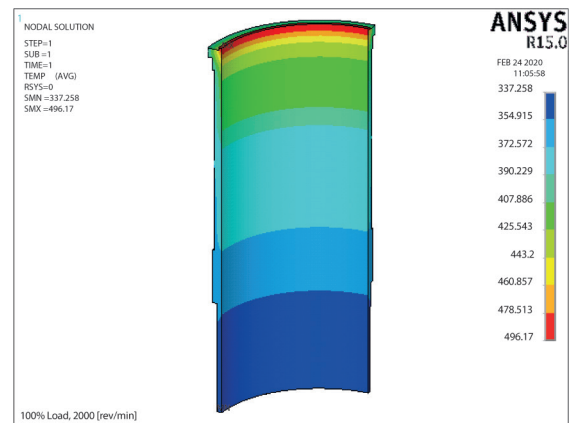

Figure 13. The cylinder liner temperature distribution at 100% load, 2000 rev/min.

the back of the liner and the temperature decreases significantly with distance from the cylinder head. These results agree well with findings present in the available literature [1] because this area is exposed to high-temperature in-cylinder burned gases. After significant gas expansion, the lower regions of the liner are only exposed to combustion products for a portion of the cycle.

Results of theoretical calculation by finite element method and comparison with experimental results at 8 survey points in the V-12 engine cylinder liner in load modes corresponding to the engine speeds of 1200 [rev/min] and 2000 [rev/min] are exhibited in table 2 and Figure 14, Table 3 and Figure 15 respectively.

Figure 14 and Figure 15 show how the temperature varies along the length and from the mirror surface to the back of a V-12 diesel engine liner at 8 survey points. The temperature distribution gradually decreases from the mirror surface to the back of the liner, and the temperature decreases significantly as one moves away from the cylinder head. At the same position, the temperature increased when increasing the load of the engine.

The comparison of theory and experiment with the V-12 engine reveals that the largest relative error is 5.49 percent at location VT8 corresponding to the survey mode at 50 percent load, 1200 [rev/min]; the most minimal relative error is 0.01 percent at location VT2 corresponding to the survey mode at 50 percent load, 1200 [rev/min].

CONCLUSIONS

The simulation and empirical values report a reasonable tendency for the cylinder thermal distribution at simulation modes. Because rising temperatures are observed as engine load increases because more fuel is required to meet the increasing load demand; thus, more energy is accessible in the engine combustion chamber.

At the various operating conditions tested, the theoretical analysis results compared favorably with the corresponding experimental ones. From the experimental results, the theoretical calculation of the temperature distribution of the V-12 engine cylinder liner is relatively accurate with the largest relative error is 5.49%. Therefore, this

Table 2. The temperature at 8 survey points in the V-12 engine cylinder liner at 50%, 60%, 75%, and 100% load at 1200 [rev/min] according to calculations and experiments

1200 [rev/min]	VT1 [ºC]	VT2 [ºC]	VT3 [ºC]	VT4 [ºC]	VT5 [ºC]	VT6 [ºC]	VT7 [ºC]	VT8 [ºC]
50%_Exp	120	108	103	96	93	92	91	89
50%_Simu	119.89	107.99	104.78	99.55	96.58	95.23	95.12	94.17
60%_Exp	122	109	105	98	95	92	92	91
60%_Simu	124.09	110.85	107.27	101.33	97.86	96.18	96.18	95.13
75%_Exp	128	111	107	100	97	95	94	93
75%_Simu	128.4	113.83	109.87	103.19	99.21	97.5	97.28	96.15
100%_Exp	130	115	113	105	99	98	97	96
100%_Simu	136.71	119.65	114.96	106.84	101.84	99.79	99.46	98.16

Figure 14. The temperature at 8 survey points in the V-12 engine cylinder liner at 50%, 60%, 75%, and 100% load at 1200 [rev/min] according to calculations and experiments.

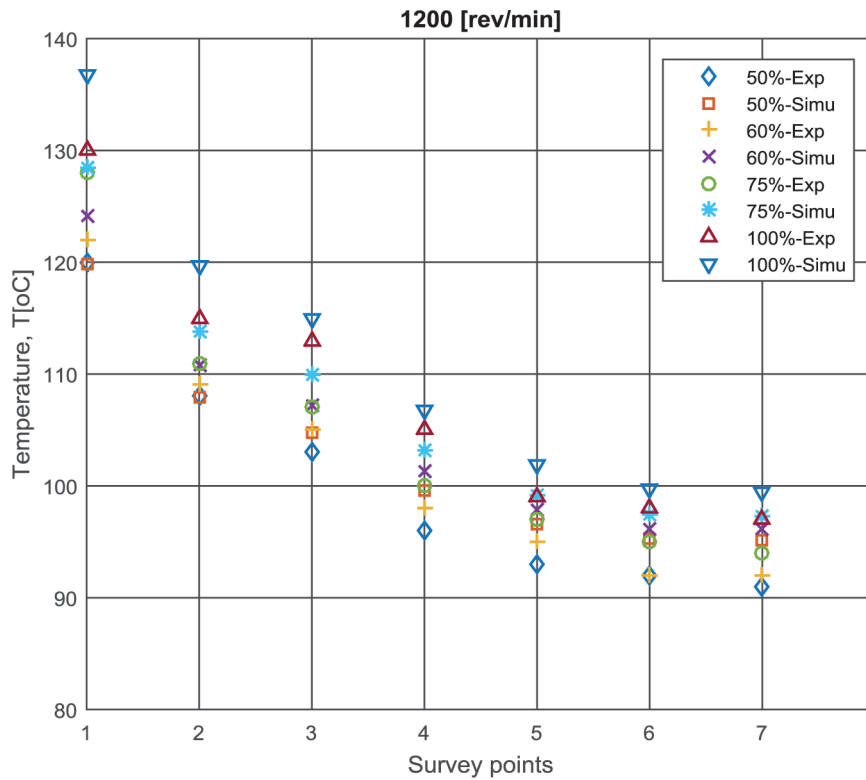**Table 3**. The temperature at 8 survey points in the V-12 engine cylinder liner at 50%, 60%, 75%, and 100% load at 2000 [rev/min] according to calculations and experiments

2000 [rev/min]	VT1 [ºC]	VT2 [ºC]	VT3 [ºC]	VT4 [ºC]	VT5 [ºC]	VT6 [ºC]	VT7 [ºC]	VT8 [ºC]
50%_Exp	124	110	108	99	95	93	93	92
50%_Simu	119.08	112.4	110.07	103.07	99.05	97.495	97.17	96.68
60%_Exp	126	112	110	101	97	95	95	94
60%_Simu	122.38	115.3	112.79	105.04	100.49	98.83	98.41	97.96
75%_Exp	130	116	113	105	100	98	97	95
75%_Simu	126.13	118.63	115.92	107.3	102.14	100.38	99.83	99.45
100%_Exp	145	133	130	117	108	105	102	102
100%_Simu	144.27	135.58	132.1	119.12	110.79	108.46	107.24	107.4

theoretical model can be used to calculate for subsequent purposes.

The calculated results of the temperature distribution are the important basis to calculate the thermal stress of the cylinder liner, which is then added to the mechanical stress field to determine the total stress distribution. Such findings can be used to specify appropriate materials in the actual cylinder liner design.

DATA AVAILABILITY STATEMENT

The authors confirm that the data that supports the findings of this study are available within the article. Raw data that support the finding of this study are available from the corresponding author, upon reasonable request.

CONFLICT OF INTEREST

The author declared no potential conflicts of interest with respect to the research, authorship, and/or publication of this article.

ETHICS

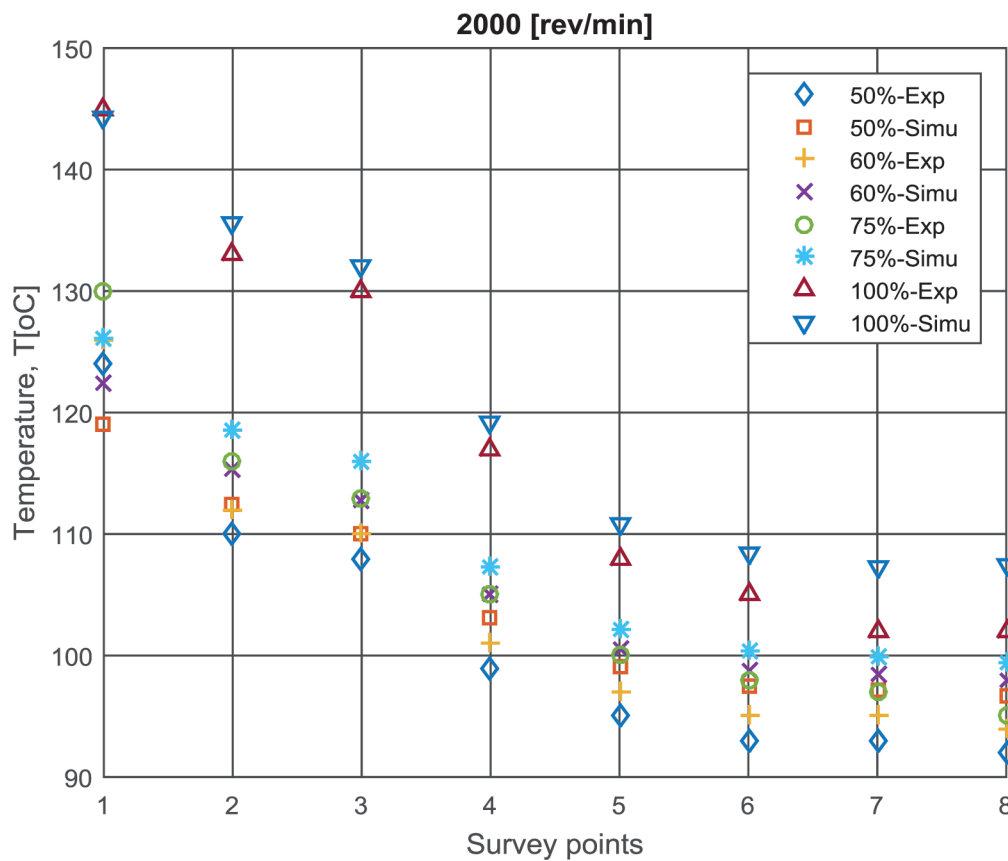There are no ethical issues with the publication of this manuscript.

Figure 15. The temperature at 8 survey points in the V-12 engine cylinder liner at 50%, 60%, 75%, and 100% load, 2000 [rev/min] according to calculations and experiments.

REFERENCES

[1] John B.Heywood. Internal combustion engine fundamentals. Second Edition. McGraw-Hill International Editions, London; 2018.

[2] Finol CA, Robinson K. Thermal modelling of modern engines: A review of empirical correlations to estimate the in-cylinder heat transfer coefficient. P I Mech Eng D-J Aut 2006;220:1765–1781. [CrossRef]

[3] Rakopoulos CD, Andritsakis EC, Hountalas DT. The influence of the exhaust system unsteady gas flow and insulation on the performance of a turbocharged diesel engine. Heat Recov Syst CHP 1995;15:51–72. [CrossRef]

[4] Kouremenos DA, Rakopoulos CD, Hountalas DT. Thermodynamic Analysis of Indirect Injection Diesel Engines by Two-Zone Modeling of Combustion. J Eng Gas Turbines Power 1990;112:138–149. [CrossRef]

[5] Sitkei G. Heat transfer and thermal loading in internal combustion engines. Mater Sci 1974: 135650801.

[6] Richardson DE. Review of power cylinder friction for diesel engines. review of power cylinder friction for diesel engines. J Eng Gas Turbines Power 2000;122:506–519. [CrossRef]

[7] Dehghani Firoozabadi M, Shahbakhti M, Koch CR, Jazayeri SA. Thermodynamic control-oriented modeling of cycle-to-cycle exhaust gas temperature in an HCCI engine. Appl Energy 2013;110:236–243. [CrossRef]

[8] Wang X, Stone CR. A study of combustion, instantaneous heat transfer, and emissions in a spark ignition engine during warm-up. P I Mech Eng D-J Aut 2008;222:607–618. [CrossRef]

[9] Rahmani R, Rahnejat H, Fitzsimons B, Dowson D. The effect of cylinder liner operating temperature on frictional loss and engine emissions in piston ring conjunction. Appl Energy 2017;191:568–581. [CrossRef]

[10] Dere C, Deniz C. Effect analysis on energy efficiency enhancement of controlled cylinder liner temperatures in marine diesel engines with model based approach. Energy Convers Manag 2020;220:113015. [CrossRef]

[11] Gustof P, Hornik A. Determination of the tempera-ture distribution in the wet cylinder sleeve in turbo diesel engine. J Achiev Mater Manuf 2008;27.

[12] Colin R. Ferguson, Kirkpatrick A.T. Internal Combustion Engines Applied Thermosciences. 3rd ed. United Kingdom, Wiley; 2016.

[13] Двигатели В-2 и В-6. Техническое описание. М.: Военное издательство. 1975.

[14]   Dewangan S.K, Naik M.P.K, Deshmukh V. Parametric study of the non-premixed coal combustion in furnace for heat transfer and emission characteristics. J Therm Eng 2020;6:323–353. [CrossRef]

[15]   Akinshilo A. Analytical Decomposition Solutions for Heat transfer on Straight Fins with Temperature Dependent Thermal Conductivity and Internal Heat Generation. J Therm Eng 2018;5:76–92. [CrossRef]

[16]   Kien NT. Research of the effect of compressor pressure ratio on thermal load in diesel engine. 2016.

[17]   Mary Kathryn Thompson, Thompson J.M. ANSYS Mechanical APDL for Finite Element Analysis. Butterworth-Heinemann; 2017.

[18]   Piotr Gustof, Hornik A. Jedrusik D. Modelling of the heat load in the piston of turbo diesel engine - continuation. Transport Problems 2007:2;81–86.

[19]   Esfahanian V, Javaheri A, Ghaffarpour M. Thermal analysis of an SI engine piston using different combustion boundary condition treatments. Appl Therm Eng 2006;26:277–287. [CrossRef]

APPENDIX

The following APDL Code is a written program for a specific case (50% load and 1200 rev/min) by The ANSYS Parametric Design Language (APDL):

```
/Title, The cylinder liner temperature distribution [50% Load; 1200 rev/min]
/FILNAME,50%Load_1200rpm
/Prep7
KEYW,Thermal,1
/PMETH,STAT,0
K,1,0,0,0
K,2,78.5,0,0
K,3,78.5,64,0
K,4,79,64,0
K,5,79,82.3,0
K,6,82,82.3,0
K,7,82,122.3,0
K,8,81,122.3,0
K,9,81,259,0
K,10,82.5,259,0
K,11,82.5,268,0
K,12,86,268,0
K,13,86,275,0
K,14,77.5,275,0
K,15,77.5,276.8,0
K,16,75,276.8,0
K,17,75,268.8,0
K,18,75,238.8,0
K,19,75,208.8,0
K,20,75,178.8,0
K,21,75,148.8,0
K,22,75,118.8,0
K,23,75,88.8,0
K,24,75,0,0
K,25,0,280,0
L,2,3
L,3,4
L,4,5
L,5,6
L,6,7
L,7,8
L,8,9
L,9,10
L,10,11
L,11,12
L,12,13
L,13,14
L,14,15
L,15,16
L,16,17
L,17,18
L,18,19
L,19,20
L,20,21
L,21,22
L,22,23
L,23,24
L,24,2
LGLUE,ALL
AL,ALL
VROT,ALL,,,,,,1,25,90,1
/VIEW,1,-2,1,1
/TYPE
ET,1,SOLID90
MPTEMP,1,20,100,200,300,400,500
MPTEMP,7,600,700,800
MPDATA,C,1,2,496,517,533,546,575,609
MPDATA,C,1,8,638,676
MPDATE,DENS,1,1,7710,7710,7710,7710,7710,7710
MPDATE,DENS,1,7,7710,7710,7710
MPDATA,KXX,1,1,33*10E-3,33*10E-3,32*10E-3,31*10E-3,20*10E-3,20*10E-3
MPDATA,KXX,1,7,28*10E-3,27*10E-3,27*10E-3
MPDATA,ALPX,1,2,11.5*10E-6,11.8*10E-6,12.7*10E-6,13.4*10E-6,13.9*10E-6,14.7*10E-6
MPDATA,ALPX,1,8,14.9*10E-6
MPDATA,ALPY,1,2,11.5*10E-6,11.8*10E-6,12.7*10E-6,13.4*10E-6,13.9*10E-6,14.7*10E-6
MPDATA,ALPY,1,8,14.9*10E-6
MPDATA,ALPZ,1,2,11.5*10E-6,11.8*10E-6,12.7*10E-6,13.4*10E-6,13.9*10E-6,14.7*10E-6
MPDATA,ALPZ,1,8,14.9*10E-6
    TUNIF,400
    SFA,16,,CONV,291.75*10E-6,783.12
    SFA,17,,CONV,275.35*10E-6,670.87
    SFA,18,,CONV,174.38*10E-6,587.50
    SFA,19,,CONV,128.79*10E-6,481.00
    SFA,20,,CONV,110.90*10E-6,430.96
    SFA,21,,CONV,102.60*10E-6,393.90
    SFA,22,,CONV,500*10E-6,352.15
    SFA,23,,CONV,500*10E-6,333.15
    SFA,2,,CONV,200*10E-6,319.65
    SFA,4,,CONV,5000*10E-6,351.15
    SFA,6,,CONV,5000*10E-6,351.15
    SFA,8,,CONV,6000*10E-6,355.15
    SFA,10,,CONV,5000*10E-6,364.15
    SFA,12,,CONV,5000*10E-6,364.15
LSWRITE,SO1
ESIZE,6
VSWEEP,ALL
FINISH
/SOLU
ANTYPE,0,NEW
NROPT,AUTO
CNVTOL,TEMP,300,0.0005
SOLVE
FINISH
```

```
/POST1
PATH,Path7,2,30,30
PPATH,1,,75,157,0,0
PPATH,2,,81,157,0,0
```

```
PSEL,S,Path7
PDEF,,TEMP
PLPATH,TEMP
PLNSOL,TEMP,,,1
```